Academic Science Journal

A Review on Development Prospect of CMTS Based Thin Film Solar Cells

Rafal A. Abdullah*, Nabeel A. Bakr

Department of Physics, College of Science, University of Diyala, Iraq

* rafl1995aa.rafl1995aa@gmail.com

Received: 23 February 2023 **Accepted: 27 November 2023**

DOI: https://dx.doi.org/10.24237/ASJ.02.04.749B

Abstract

CMTS is a quaternary semiconductor similar to copper zinc tin sulfide (CZTS) which is non-toxic and abundant on Earth and is a P-type light absorbent material which is suitable for thin-film solar cell fabrication and achieves better conversion efficiency of 0.78% , as well as having a direct energy gap estimated at (1.76 eV) and a high optical absorption coefficient [20] ($\alpha \geq 10^4$ cm^{-1}). In this paper, the development cases of a Cu_2MgSnS_4 composite in the thin-film industry, as well as its use in solar cell applications, are summarized. Illustrated and explained the difficulty related to processing the raw material, the manufacturing procedure, and manufacturing equipment. Finally, the potential for development of Cu_2MgSnS_4. Where the focus was on thin films.

Keywords: Quaternary chalcogenide, Quaternary, Synthesis techniques, Zinc buckle, Stannite structure, Kesterite structure, Cu_2MgSnS_4.

مراجعة لآفاق تطوير الخلايا الشمسية ذات الأغشية الرقيقة المعتمدة على CMTS

رفل علي عبدالله, نبيل علي بكر

قسم الفيزياء - كلية العلوم - جامعة ديالى

الخلاصة

CMTSعبارة عن شبه موصل رباعي يشبه كبريتيد القصدير والخارصين النحاسي (CZTS) وهو غير سام ومتوفر على الأرض وهو مادة ماصة للضوء من P-type مناسبة لتصنيع الخلايا الشمسية ذات الأغشية الرقيقة وتحقق كفاءة تحويل

Academic Science Journal

أفضل بنسبة 0.78% ، بالإضافة إلى وجود فجوة طاقة مباشرة تقدر بـ (1.76 eV) ومعامل امتصاص بصري مرتفع (cm^{-1} $\alpha \geq 10^4$). في هذا البحث ، تم تلخيص حالات تطوير مركب Cu_2MgSnS_4 في صناعة الأغشية الرقيقة ، وكذلك استخدامه في تطبيقات الخلايا الشمسية. تم توضيح وشرح الصعوبة المتعلقة بمعالجة المواد الخام وإجراءات التصنيع ومعدات التصنيع. أخيرًا ، إمكانية تطوير Cu_2MgSnS_4 كان التركيز على الخلايا الشمسية ذات الأغشية الرقيقة.

الكلمات المفتاحية: الكالكوجينيد الرباعي، الرباعي، تقنيات التخليق، إبزيم الخارصين، التركيب الستانيتي، التركيب الكستيري، Cu2MgSnS4.

Introduction

The development and use of solar cells have drawn attention from all over the world due to the rising use of conventional energy and the escalating environmental catastrophe. The development of thin film preparation techniques over the last ten years has encouraged the development of 2nd generation solar cell using semiconductor-based thin-film material. The solar cell thin film technique could significantly lower the cost of materials because it requires less material. Additionally, the thin films can easily be applied to a variety of substrates, includes plastic, stainless steel, and glass, making them particularly useful for the integration of solar panels into buildings. cadmium telluride (CdTe), Amorphous silicon thin film, and copper indium selenium (ICIGS cell) are now the three primary types of thin film solar cells (CIS), the gallium arsenide, copper indium gallium selenium CI(G)S or CIS cell), and the copper zinc tin sulfur (Cu_2MgSnS_4 is mentioned to below to as CMTS). Hazardous elements (cadmium and arsenic) are present in gallium arsenide and cadmium telluride, while the system copper indium gallium selenide includes uncommon indium elements, these kinds of solar cell fall short of anticipated advancements in solar technology.

Thin films have been studied as suitable absorber materials for highly efficient solar cells Cu2ZnSnS4 (CZTS). [1, 2]. Cu_2ZnSnS_4 CZTS based solar cell have shown a promising competence of 12.6 %, but this is still below the theoretical limit of more than 30% [3]. The performance of the equipment is primarily restricted with the production phases with impurities and a significant number of CuZn antisite defects. It was discovered that replacing Zn with other elements was a successful approach for increasing efficiency [4]. Then, Cu_2MSnS_4 (M=

Cd^{2+} , Fe^{2+}, Ni^{2+} and Mn^{2+}) Additionally, using a variety of techniques, thin film with acceptable photo-electrical characteristics was created. It is noteworthy that the Cu2CdSn(S,Se)4 and Cu2MnSnS4 solar cells showed respective efficiency of 3.1% and 0.91% [5, 6]. However, Mn will introduce unwanted magnetism into the electronics, and Cd is a poisonous metal.

Earth-abundant Mg element-containing quaternary compound Cu2MgSnS4 (CMTS) may be an absorbent substance that is acceptable to the environment. Wei et al. employing the hot-injection method, CMTS nanoparticles having a 1.67 eV energy band gap were first created. The major diffraction peaks agree well with the predicted patterns of the kesterit CMTS structure, leading them to hypothesize that the nanoparticles have a kesterite structure [7]. But a first-principles analysis suggested that The CMTS's kesterit structure is unstable since it spontaneously disintegrated. [8, 7]. Guo et al. co-spray pyrolysis was used to create CMTS thin films, with bandgaps of 1.76 eV, which showed that the CMTS film has grown closely resembled a tetragonal structure [9]. The importance of post-sulfuration in the creation of high quality chalcogenide thin film is well known, still little research has been done on how the annealing technique affects the characteristics of CMTS films.

Bell Lab successfully fabricated Cu2CdSnS4-based monocrystalline solar cells in 1977, and they had an efficiency of 1.6% [10]. Japan's Nakazawa and Ito In 1988, Shinshua University produced a Cu_2CdSnS_4 mono-crystal and used it to attain a 165 mV open circuit voltage [11]. Kategiri et al. synthesized p- type conductivity in 1997 and attained a conversion efficiency of 0.66% with an absorption coefficient over 10^4 cm^{-1} and a band gap of 1.45 eV [12,13]. The band structure, the kind of defect, and other aspects of single-phase based CZTS have not made any significant advances in recent years due to the limited range of their existence and the difficulty of quaternary synthesis. Investigations are ongoing.

CuInSe2 cells have recently exceeded 10% component efficiency and met a particular level of industry expectations. As the size of tablet displays increased, indium resources became rare, so researchers focused more on CZTS. The United States' leading provider of CIGS PV modules, Solyndra Company, filed for bankruptcy after Veeco of CIGS apparatus makers left

industry in 2011 (August) due to an excessively protracted time of commercialization and cost reduction. So the CZTS gained greater attention.

Crystal structure of CMTS

One of the three structural phases may be adopted by quadrilateral I-II-IV-VI semiconductors produced by cation mutational of $CuInSe_2$-like I-III-VI compounds. (Fig.1), i.e the kesterit structure, the initial mixed CuAu-like structure (PMCA), and stannite structure (ST) by space group of I42m (KS) by the space group of I4. While the chalcopyrite structures served as basis for the first structure, the last two are produced from a structure similar to CuAu. In order to investigate the fundamental structures of $Cu_2CaSnSe_4$(CCTSe), $Cu_2MgSnSe_4$ (CMTSe), Cu_2CaSnS_4 (CCTS), and Cu_2MSnX_4 (CMTS), above structures were taken into consideration.

Table 1: Calculated total energies (meV per unit cell) for Cu2MSnX4 (M=Zn, Mg, and Ca; X=S and Se) in relation to the most stable phase among Ks, ST, and PMCA [14].

SYSTEM	E_{KS}	E_{ST}	E_{PbICA}
CZTS	0	47.0	66.4
CMTS	40.2	0	95.9
CCTS	543.8	0	694.9
CZTSe	0	80.4	131.1
CMTSe	42.1	0	148.5
CCTSe	536.0	0	754.5

Derived from total energies estimated using the HSE functional (Table 1), PMCA is shown to be the least stable of these three structures. The findings supported prior calculations demonstrating that the KS structure is how compounds containing zinc's ground state are structured [14]. However, Compounds based on magnesium and calcium are both stabilized in the ST phase, which is comparable to other substitutes generated by big size atoms like Cu_2CdSnX_4 and Cu_2HgSnX_4 (X=S and Se). According to Chen's findings, For CZTS, the difference in energy between KS and ST is 47.0 meV per unit cell, but for CZTSe, it is 80.4 meV per unit cell [15]. The energy difference between ST and KS in CMTS and CMTSe is, respectively, 42.1 and 40.2 meV per unit cell. Yet, this energy disparity has led to a considerable increase in the CCTS and CCTSe. For CCTSe and CCTS, this value reaches 536.0 and 543.8

meV for every unit cell, correspondingly. Since the energy difference between CMTS and CMTSe is ST and KS phases is comparable to that of CZTS, they may be stable at thermodynamic equilibrium (See Fig. 1.) . The crystal structure shows that despite the two structures having a tiny total energy difference, there could be a significant number of antisite defects. Based on the overall energy difference value shown for (Table 1) for Zn-based materials, The simple production of PMCA secondary phase or [ZnSn+ SnZn] associated defect complex is suggested by the low total energy difference between the KS and PMCA phases in CZTS at high temperatures. Due to the relatively substantial total energy differences between the ST and PMCA structures, the PMCA secondary phases in Mg-based materials cannot simply form in both CMTS and CMTSe. Because Ca has a much higher atomic radius than Cu, it can provide a strong mechanical stress in Ca-based materials and prevent forming [CaCu +CuCa] complexes. In order to inhibit PMCA secondary phases and [CaSn+SnCa] deficiency complex, the total energy differential between ST and PMCA widens.

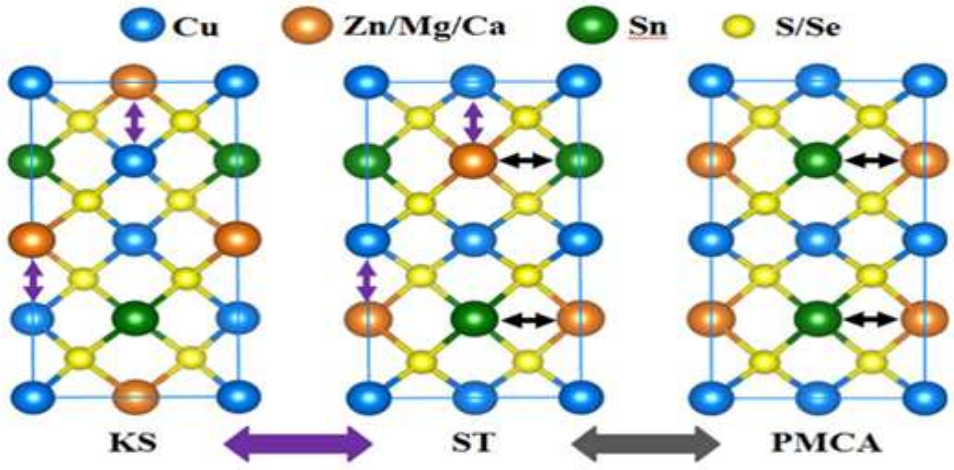

Figure1: Cu2MSnX4 can be configured into different ways: KS, ST, PMCA (M=Zn, Mg, and Ca; X=SandSe)

The [ZnCu+CuZn] defective complex that causes the reciprocal change among ST and KS structures are indicated by the purple arrows. The [SnZn+ZnSn] defective complex that causes the mutual transition between PMCA and ST are indicated by the black arrows.

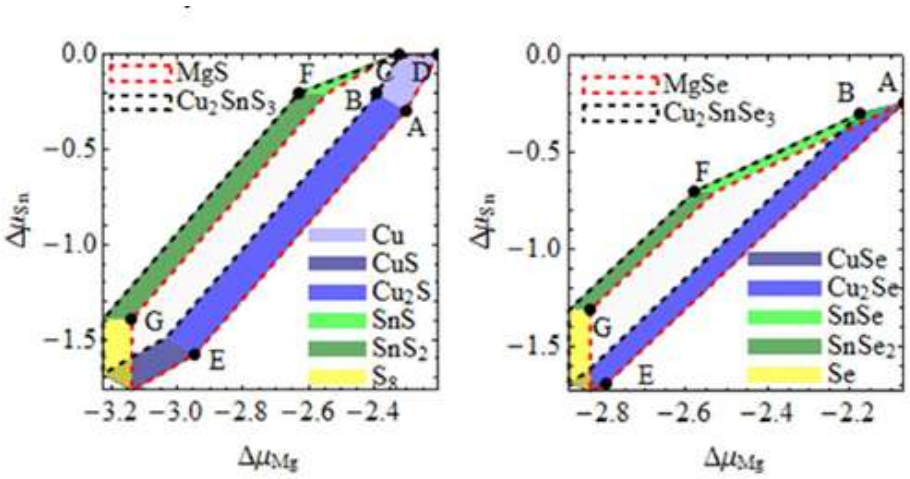

Figure 2: Phase diagram for CMTS and CMTSe shown. The front surface of the big surface bound by Cu_2SnS_3 (Cu_2SnSe_3) and the back surface of MgS (MgSe). Plotted at the Cu-richest limit (A-D), Cu-mild range (E-F), and Cu-poorest limit are indicators of Cu-chemical potential (G).

When Mg replaces Zn in the ground- state structures of Cu2MSnX4 (M= Mg, Zn, and Ca; X= Se and S), expansions in a and b direction occur. The bond length of dM-X and dCu-X are seen to rise with M atomic radius from the atomic distances. With the exception of CMTSe, the substitution results in a shrinkage in the c direction, which could be connected to the bond length decrease of dSn-X in Ca- and Mg-based compound. For Ca- and Zn- based materials, While it is essentially optimal (u=0.25) for Mg-based compounds, the anion (Se or S) displacement parameter u notably deviates from the ideal value of 0.25. In experiments, Secondary and tertiary impurities are more stable phases considerably result in a lack of stable quaternary phases or a reduction in the crystallinity of quaternary compounds. To give instructions for their synthesis, we have additionally looked at The above-mentioned materials' thermodynamic stability. The range of chemical potentials is constrained by the necessity that Cu_2MSnX_4 phase

(M= Mg, Zn, and Ca; X=S and Se) be more stable than any secondary phases in thermodynamic equilibrium. To satisfy the constraint, it is necessary that

$\Delta H_f (Cu_2MSnX_4) = 2\mu_{Cu} + \Delta\mu_M + \Delta\mu_{Sn} + 4\Delta\mu_X$, …… (1)

And for any secondary phases

ΔH_f (secondary phases) $> \sum_i n_i \Delta\mu_i$ …… (2)

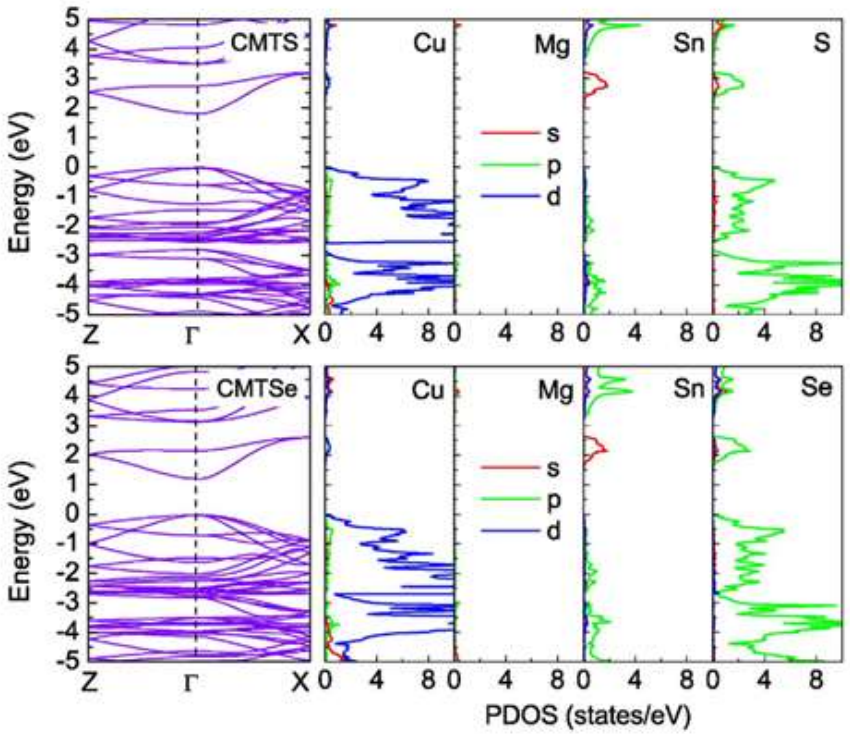

Figure 3: (Color online) Calculated band structures and projected density of states (PDOS) for ST Cu_2MgSnS_4 (top) and $Cu_2MgSnSe_4$ (bottom) [16,17].

Where ΔH_f The standard refers to the enthalpy of formation in the comparable phase, and μi and ni refer to the number of atoms and chemical potentials of the associated element [23]. Just 3 of the 4 chemical potentials are independent due to the restriction imposed by Eq. (2) . Then, by agreement, The chemical potential of the metallic components is selected as the independent variable. Obviously, any Δμ must be smaller than 0 to prevent element separation. Dimers and

ternaries further limit the variety of chemically stable potentials in the account, element of Cu, M= Mg / Zn / Sn, Ca and X= Se / S, Kesterite sulfides and selenide, CuX, MX, Cu_2X, SnX_2, SnX,and ternary compounds Cu_3SnX_4, Cu_2SnX_3 [16,17] are the subsequent phases taken into consideration.

Although copper vacancy is probably a contender for p-type conductivity, the volume of stable chemical potential is used To indicate the likelihood of generating the Cu2MSnX4 material. When the HSE exchange-correlation function is employed, the ternary phase Cu3SnX4 does not affect the border of the stable chemical potential range. The term "ecosystem" refers to a group working in the construction industry. Ca-based compounds are unstable with regard to their secondary phases, whereas Mg-based compounds have a volume of permitted chemical potential that is 40–50% of Zn-based compounds. Mg-based compounds have a somewhat lower copper limit than their Zn-based equivalents. It is thermodynamically advantageous if Cu2SnX3 and MgX can be mixed to generate Cu2MgSnX4.

$$\Delta Hf\ (Cu_2MgSnX_4) \leq \Delta Hf\ (MgX) + \Delta Hf(Cu_2SnX_3) \quad \ldots\ldots\ldots\ldots\ldots\ldots (3)$$

Even when the entropy effect is ignored. Previous work [18] Owed to GGA's failure to accurately assess the ground stat energies of Cu_2MgSnS_4, and Cu_2SnS_3, employing GGA functional has not been able to show the stable thermodynamic range of Cu_2MgSnX_4. For example, a Cu_2MgSnS_4 formation energy has increased by 0.98 eV when the GGA result is compared to the HSE result. The material's internal tension is probably the cause of the comparatively lower volume of allowable chemical potential aimed at Mg-based compounds. Due to the comparable lattice constants of ZnS (ZnSe), Cu2SnS3 (Cu2SnSe3), and CZTS (CZTSe), the bond length between Zn and S (Se) in CZTS(Se) is almost identical to that in the binary ZnS (ZnSe) compounds. As a result, internal tension surrounding Zn components is predicted to be minor in these combinations. Halite-structured materials are more stable energetically CaS(Se) and MgS(Se), in contrast, is produced by the ionicity of Ca and Mg and have substantially longer bonds and a greater coordination number than the equivalent zinc blende. Compounds based on magnesium are possible to include further strained atoms. For CMTSe, and CMTS this internal stress may result in a comparatively smaller stable chemical

potential range. Though, we must added examine their electrical and optical characteristics and contrast them with those of Zinc based material in order to assess CMTS and CMTSe's potential as photovoltaic materials. As shows in Table 2. E_g is significantly understated by GGA. We replicate the experimental E_g of CZTSe and CZTS using HSE hybrid functional [19,20]. With predicted E_g of 1.16 eV and 1.80 eV, respectively, ST structured CMTSe and CMTS are direct E_g materials and have proportionally greater E_g than CZTSe and CZTS. The larger E_g of 1.62 eV for CCTSe and 2.13 eV for CCTS seen in Ca-based materials is primarily the result of higher hybridization interactions between X-p and Sn-s statuses in addition to get less coupling interactions between X-p and M-d states. The nature of the valence or conduction band, as well as the electronic states nearby to the Fermi level, are unaffected by replacement of magnesium, according with respect to the band structures and projected density of statuses (PDOS) in Figure 3..The first-group transmission bands are primarily derived from the mixing of S-3p and Sn-5s (Se-4p) electronic states, whereas the valence bands are primarily derived from the hybridization of Cu-3d and S-3p (Se-4p) electronic states. When compared to Zn-based materials, the bond length reduction increases the interaction among Sn and S (Se), which is what causes the slight rise in E_g in magnesium -based materials.

Table 2: shows the computed band gap for Cu_2MSnX_4 (M=Zn, Mg, and Ca; X=S and Se), the optimal lattice constant, the anion displacement parameter u, and the closest atomic distance. a Ref. [19,21]. b Ref. [22]. c Ref. [23,20]

							EG (EV)		
system	a (A)	c (A)	u	dcu-x (A)	dm-x(A)	dsn-x (A)	Expt.	GGA	HSE
CZTS (KS)	5.475	10.943	0.25±0.0157	2.321(2.325)	2.370	2.471	1.4-1.6a	0.09	1.60
CMTS (ST)	5.568	10.932	0.25 ±0.0006	2.330	2.471	2.464	1.63b	0.19	1.80
CCTS (ST)	5.903	10.483	0.25 ±0.0206	2.363	2.726	2.449	-	0.55	2.13

CZTSE (KS)	5.771	11.537	0.25 ±0.0183	2.437(2.444)	2.449	2.623	0.95-1.05c	0.02	1.00
CMTSE (ST)	5.864	11.562	0.25 ±0.0006	2.447	2.611	2.617	-	-0.05	1.16
CCTSE (ST)	6.173	11.186	0.25 ±0.0185	2.476	2.859	2.602	-	0.18	1.62

Table 3: Listing of copper chemical potential limit and volume of stable chemical potential range for Cu_2MSnS_4 and Cu_2MSnSe_4 (M=Zn, Mg, and Ca) showing that replacement of Zn by Mg forms energetically stable compound [24].

	M=MG	M=ZN	M=CA
Quaternary sulfide μCu range (eV)	-0.72/0	-0.67/0	Unstable
Quaternary selenide μCu range (eV)	-0.65/0	-0.62/-0.01	Unstable
Volume of stable chemical potential of Cu2MSnS	0.076	0.038	-
Volume of stable chemical potential of Cu2MSnSe	0.057	0.023	-

Energy band structures of CMTS.

The lack of knowledge of fundamental arrangement and crystal structure makes it challenging to undertake research on electrical, optical, and other characteristics. For solar cell materials, it is essential to have electrical properties such as energy band width, state density, doping behavior, and transport attributes. Table 3 demonstrates that, Even though there are some oddities in the various theoretical answers for the energy gap of Cu2ZnSnS4 and Cu2ZnSnSe4, the band gap of sulfide is larger than that of selenide.

If the ratio of selenium to selenium and selenium is reported as X for CZTS doped with selenium, it could be represented as

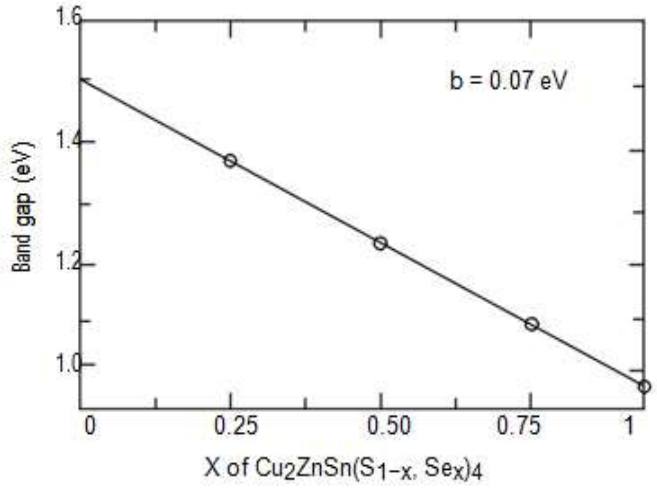

Figure 5: Varying diagram of $Cu_2ZnSn(S_{1-x}, Se_x)_4$ band gap with x adapted from [24].

$Cu_2ZnSn(S_{1-x}, Se_x)_4$, and it's band gap can be adjusted as of 1.0 eV to 1.5 eV:

$$Eg\ (X) = (1-x)\ (CZTS) + (CZTSe) - bx\ (l-x). \qquad \text{.....(4)}$$

When b equals 0.07, we may get the Cu2ZnSn(S1x, Sex)4's variable band gap diagram with x, as illustrated in Figure 5.

Preparation Methods of CMTS Thin Film.

1. Method of electrochemical deposition. Electrochemical deposition or hot-dip liquid in cathode, which materials potential difference with external circuit power, is a coating process to lessen the cations in an organic or aqueous explanation. People instigated experimenting with semiconductor material electrochemical deposition in the 1970 s.[25,26].

These days, solar cells are often made using the electrodeposition approach, such as the CIGS solar cells created with France's CISEL [27] and the CdTe cells made via BP plc [28]. Although thiourea was utilized as a precursor for the electrodeposition of CdS [29], Finding a reliable sulfur supply for the electrodeposition of CZTS proved challenging. As of 2008, the Bath University in the UK's electrodeposition Cu/Sn/Zn technique allowed the CZTS solar cells to attain a conversion efficiency of 0.8%. [30,31].

In 2010, Through the use of enhanced technology, they were able to produce the cells tool by a alteration efficiency of 3.2% by hardening for two hours at 575℃ in an environment of N_2 carrier gas containing S powder and 10% H_2 [32]. In 2009, By electrodepositing a Cu/Sn/Zn laminate, Nagaoka University of Technology verified a conversion efficiency of 0.98%. The laminate was then heated to 600 degrees Celsius for two hours in a transportation gas involving sulfur powder. Before electro-deposition, a Pb sheet was deposited on Mo to improve the substrate adherence [33]. They were able to created solar cells with a conversion efficiency of 3.16% after annealing for two hours at 600 °C in a carrier gas containing sulfur powder. [34].

The same year, German national Ennaoui HZB developed CZTS solar cells with a 3.4% photovoltaic conversion efficiency utilizing the one-step codeposition of CuZnSn in a solution containing 3 mM Cu2+, 3 mM Zn2+, 30 mM Sn2+, and some complexing agent. After that, the cells were kept in an atmosphere of Ar gas with 5% H2S and CZTS films for two hours at 550 °C. Its effectiveness rose to 3.6% after 10 minutes of light therapy. [35,36].

In 2012, In order to progressively layer a Cu/Zn/Sn laminate, IBM used a commercial plating solution. It was then annealed for 30 minutes at 350 °C in N2, made into a CuZnSn alloy, and then annealed for 12 minutes at 585 °C in N2 containing sulfur powder [37]. This resulted in CZTS solar cell by an efficiency of 7.3%. A unique chemical SILAR (succeeding ionic layer adsorption and reaction) approach was recently created by Shinde et al. [38] for the sequential reaction-based synthesis of CZTS thin film on the surface of SLG substrates. The substrate was gradually submerged in a beaker containing the cationic precursor solutions of 0.1 M CuSO4, 0.05 M ZnSO4, and 0.05 M SnSO4 (1: 1: 1) and the anionic precursor solution of 0.2 M thioacetamide for the production of CZTS thin films. The final films were then annealed at 400 °C for 4 hours.

The annealed CZTS thin film was used to build 0.12% efficient photoelectrochemical solar cell (PEC) cell Mali et al. [39] fabricated CZTS thin films based solar cells with a conversion efficiency of 0.396% using a similar process. The authors neglected to note the device's poor efficiency, which was brought on by the high contact resistance. Subsequently, the same team

of researchers employed a comparable method to raise the efficiency of solar cells built using CZTS thin films to 1.85% [40].

The CZTS thin film solar cell's greatest efficiency to date was attained using the wet chemistry (SILAR) method. A unique method aimed at CZTS thin films based solar cells that utilises oxide precursors via an exposed atmosphere chemical vapour deposition was recently disclosed by Washio et al. [41]. (OACVD). CZTS thin films were produced by sulphurizing oxide precursor thin films (Cu-Zn-Sn-O) in a N2 + H2S (5%) atmosphere at 520-560 °C for three hours on Mo and SLG crusted SLG substrates.

Efficiency for the best solar cell was 6.03%. The advantages of thin films fabrication by electro-deposition is low temperature statement, good interface bonding, and the absence of residual thermal pressure among the coating and substrate. The ability to produce a homogeneous thin layer over various surfaces, including those with complicated forms and porous surfaces, as well as the ability to precisely manage the coating thickness, chemical composition, structure, and porosity, are advantages.

2. Pyrolysis Deposition via Spray. In 1997, Nakayama and Ito published a paper on the spray pyrolysis technique deposition of precursor solutions in ambient environment to manufacture CZTS thin film. An adequate quantity of a predecessor solution including $ZnCl_2$, CuCl, SnCl4, and thiourea in a deionized water/ethanol solvent combination was scattered over a animated SLG substrate. The deposition film was of the stannite variety[42]. Since then, various precursor solutions have been employed in a similar manner by other researchers to fabricate CZTS thin films. Kamoun et al. examined how substrate temperature and the spray time affected the crystallinity of the CZTS films. The substrate temperature of 613 K produced the best crystallinity, and the film showed a preferred orientation along the (112) plane [43]. Kumar et al. additionally looked at the impact of the substrate temperature, pH level, precursor solution compositions, and predecessor solution composition on the morphology and crystallinity of the CZTS material. According to their findings, a CZTS material with respectable crystallinity may be produced at a substrate temperature between 643 and 683 K by a precursor

solution pH of 4.5. But in addition to the CZTS molecule, impurities including ZnS were found. [44,45]. CZTS thin films were deposited on an SLG substrate using the ultrasonic spray pyrolysis approach developed by Prabhakar and Nagaraju. At 613 K, films with a kesterite structure were produced, which is consistent with the findings of previous researchers [46].

In 2022, Using methanol as a solvent and depositing Cu2MgSnS4 thin films on glass substrates at various temperatures (150, 175, 200, and 250 °C), Souli et al. explored the production of Cu2MgSnS4 thin films using the chemical spray decomposition approach. According to X-ray diffraction analysis, vacuum hardening at 450 °C completely eliminated the secondary phases and increased the particle magnitude to 51.82 nm for the produced films. The energy gap energy varied from 1.33 eV to a maximum value of 1.91 eV with an absorption coefficient of. (105 cm-1) [47].

In 2022, Hammoud et al. studied the effect of sulfur concentration on Cu_2MgSnS_4 thin films by spray pyrolysis method, deposited on glass substrates. For all sulfur concentrations, according to XRD results, CMTS thin films crystallized in the dominant face (112) Kesterite phase with several secondary phases. The grain size values of the prepared CMTS thin films differ depending on the [S] values, the Raman spectroscopic diagnosis confirmed these results, as two distinct peaks appeared at (287-331 cm^{-1}), the SEM microscopic images showed different textures, as the surface morphology depends on the S concentration] with the presence of nanospheres when the S concentration was increased[48].

3. CZTS Precursor Solution Spin-Coating. The spincoating process is commonly used to create a CZTS thin film in three steps. The first step is to create a precursor solution with the necessary ions. In steps two and three, the solution is spin-coated onto an SLG substrate to produce a thin film, and in step three, the thin film is appropriately annealed to produce CZTS materials.

Tanaka and associates spun-coated a precursor sol-gel solution to produce CZTS films. The precursor solution included 2-methoxyethanol as a solvent and the chloride acetate salts of

copper (II), zinc (II), and tin (II). In order to avoid precipitation, monoethanolamine was added to the mixture. By annealing the precursor films at 500 °C in an environment containing H2S, CZTS thin films were created [49]. The CZTS layer was the only component of thin film solar cells not created using vacuum methods, according to a subsequent research. The CdS buffer layer was created using a chemical bath deposition technique, whereas the Zn/ZnO: Al window layer was created using a spin-coating technique. The efficiency of the non-vacuum processes used to create CZTS solar cells is 1.01% (Jsc = 7.8 mA/cm2, Voc = 390 mV) [50]. The relationship between the form and optical properties of the CZTS thin films and the precursor solution's chemical makeup was investigated. The films made from the copper-poor precursor solution (Cu/(Zn+Sn) = 0.8, molar ratio) were shown to contain large granules. The band gap energy of the copper-deficient films was greater than that of the copper-rich films. The efficiency of the highest solar cell was 2.03% [51].

Pawar et al. examined how the complexing agent trisodium citrate affected the CZTS thin films' shape, composition, and structure in the precursor solution. The outcomes demonstrated that employing the complexing agent increased the films' crystallinity. The surface of the precursor films was uneven in comparison to the films that were deposited from the electrolyte without the complexing agent. This impact was lessened by treating the films after sulfurization [52]. Ethylxanthate was also added by Liu et al. to assist make a homogeneous CZTS precursor solution that was used to deposit CZTS films [53].

By spin coating a precursor solution including thioacetamide in pyridine and the metal salts of copper (I), tin (IV), and zinc, Fischereder et al. were able to create CZTS films (II). They found that the CZTS compound may form in vacuum at as little as 105 °C. The films' band gap energy varied between 1.41 and 1.81 eV by varying the annealing temperature point [54]. The secondary phases coexisting in the film at the low annealing temperature is most likely what is causing this.

The Cu, Sn, Zn, and S elements in a particle-solution slurry of hydrazine served as the foundation for the CZTS precursor developed by Todorov et al. The precursor films were converted into CZTS films or partially selenized CZTS (CZTS/Se) thin films by hardening them

at 540°C in a sulfur or sulfoselenide containing atmosphere. The film presented large granules and a uniform composition (Figure 6(a)). The greatest cell efficiency, 9.66%, was found in solar cells having a CZTS/Se basis. Figure 6(b) of the IPCE spectrum for the thin film solar cells revealed that the photon response began at about 1200 nm, indicating that the materials had a lower band gap energy [55].

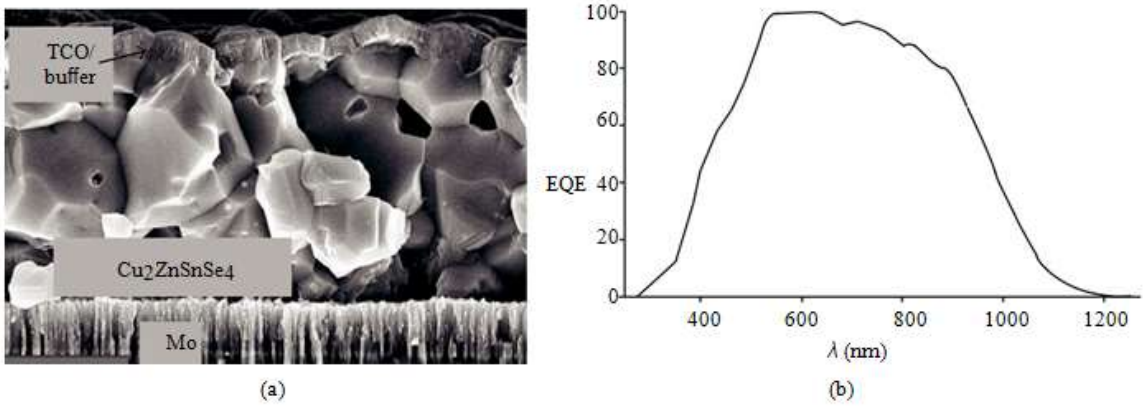

Figure 6: SEM of cross section and EQE of thin film solar cells based on CZTSSe light absorber [55].

4. Hot-Injection CZTS Nanocrystal Production. The hot injection solution chemical process is a proven method for creating objects with precise size and shape (nanocrystals). It has been extensively used in the production of semiconductor nanocrystals. 2009 saw the publication of three researchers on the hot-injection technique for the synthesis of CZTS nanocrystals in the Journal of the American Chemical Society. The materials used to create the nanocrystals had a reduced band gap energy and were less than 20 nm in size . The band gap energy of the nanocrystals was close to 1.5 eV, matching that of the bulk substance [56–58].using the hot-injection technique, Kameyama et al. looked at how the reaction temperature impacted the development of CZTS nanocrystals. They found that while single-phase CZTS was produced at temperatures over 240°C, secondary phases like CuS were produced at low reaction temperatures. In comparison to Ag/AgCl, the produced films' valence band and

conduction band were 0.3 eV and 1.2 eV, respectively [59]. By changing the chemical make-up of the heated chemical solution, the band gap energy of the nanocrystals was reduced from 3.48 eV (ZnS) to 1.23 eV. (CZTS, sphalerite kind). The efficiency of CZTS nanocrystals in dye sensitized solar cells was exceedingly low (0.03%), according to research [60]. On the other hand, when CZTS nanocrystals were hardened in Se vapour for 15 minutes at 500 °C, grain growth was sped up. The CZTSSe light absorber-based thin film solar cells had an energy conversion efficiency of 7.2%, and a one month light soaking test found no noticeable cell degradation in the band gap energy from 3.48 eV (ZnS) to 1.23 eV. (CZTS, sphalerite type)[61].

CZTS typically has a tetragonal structure and can be found in the kesterite or stannite phases. Lu et al. recently created CZTS nanocrystals with wurtzite phase utilizing the hot-injection method. The newly discovered structure is hexagonal and displayed a band gap energy of 1.4 eV [62].

In 2014, Wei et al. studied the preparation of Cu_2MgSn_4 thin films by hot-injection method, and using X-ray diffraction, Raman spectroscopy, and electron microscopy found that the prepared CMTS nanoparticles were of pure Kesterite phase. It was found, by diagnosing the surface topography, that copper, magnesium, tin, and sulfur are uniformly distributed. Cu_2MgSnS_4 nanofilms have an optical energy gap of 1.63 eV, which is appropriate for use in the field of photovoltaics, according to the UV-visible absorption spectra [63].

5. Pulsed Laser for Deposition Technique. The substrate is deposited as a result of the plasma emission's directional local area expansion and thin film formation. Using the pulsed laser deposition technique, the high power pulse laser is focused on the target surface to produce high temperatures and cauterization before creating high pressure and high temperature plasma. Moholkar and others Grinding produced the Cu2S, ZnS, and SnS2 powder, which was then transformed into a CZTS target by a solid state reaction. A CZTS thin layer was deposited on the target after it had been hit by an excimer laser beam, and it was then annealed in an environment of N2 + H2S gas. A band gap of 1.52 eV, an open circuit voltage of 585 mV, a short circuit current density

of 6.74 mA/cm2, a fill factor of 0.51, and a conversion efficiency of 2.02% were all characteristics of the thin film cells produced using this technology. The study found that the grain size increased with increasing pulse frequency when the laser pulse frequency was between 2 and 10 Hz. We were able to create homogenous, single, and dense crystal grains as a result of the laser's high energy density and the improved crystallization proces [64].

This approach is particularly well suited for depositing multicomponent heteroepitaxial films and metal oxide thin films because it is simple compared to other techniques and can deposit the film with the optimum stoichiometric ratio. The ceramic target's composition and oxygen pressure are both under control. Additionally, the strong laser beam bombardment's high energy atom or molecule bombardment of the target facilitates the deposition of high-quality thin films at low temperatures.

6. Sol-Gel Technique. Sol is produced by the reactions of hydrolysis and polycondensation of easily hydrolyzable metal compounds (inorganic salts or alkoxides) by water in certain solvents, such as dipping or spin-coating. Sol can be heated to turn it into amorphous (or crystalline) films after gelatinization. The three procedures commonly involved in the manufacture of thin films using the spin-coating method include preparing a precursor solution comprising a specified ion, spin-coating the solution onto a glass substrate to generate a film, and finally annealing thin films in the proper environment.

Sol gelatin was developed in 2007 via Tanaka et al. at Nagaoka University of Technology by means of cuproic, zinc, and tin acetates. It was then coated on Mo glass using dimethyl alcohol as the solvent and ethanolamine as the stabilizer. Before being torched at 300 °C for five minutes in air and then annealed a second time for an hour at 500 °C in an atmosphere of N2 gas containing 5% H2S, the spin coating must be performed five times to get the desired thickness. Eventually, a CZTS thin film with better a components and crystallinity was produced[65].

In 2009, A 0.35 M sol could be spun-coated and dried three times, a 1.76 M sol could be spun-coated and dried five times, and ultimately a CZTS film with a uniform surface and an efficiency of 1.01% could be produced [66]. They were able to reach a conversion efficiency of 2.03% in 2011 [67] by improving the film's component sections. In 2009, Guo et al. from Purdue University produced CZTS films and 16 nm CZTS nanoparticles using hot infusion and dropping coating, respectively. A conversion efficiency of 0.8% was attaine [36].

In 2010 They attained a conversion efficiency of 7.2% [68] via knife coating, and for a month after illumination, the cells showed no sign of recession. The cells that at the time had the highest efficient CZTS are those that IBM spin-coated the hydrazine solution using in 2010 to reach a conversion efficiency of 9.6% [69] [70, 71]. The conversion efficiency was raised to 10.1% using the MgF2 antireflection layer [72]. Its various unique advantages versus substitute techniques include: On a substrate, a large area of thin films in various shapes and materials may be produced without the need of costly equipment or vacuum conditions. A homogeneous, multicomponent oxide film with uncomplicated quantitative doping and effective composition and microstructure control is basic to create. The price of raw materials is costly, and some of them are hazardous organics. Usually, the complete process takes longer (mainly referring to the aging period). The gelatin contains a lot of micro-gel pores, which enable a lot of gas and organics to escape during the drying process and cause contraction.

In 2019 Gang Yang et al. The impacts of sulfuration, spin coating, and the creation of Cu2MgSnS4 thin films were examined, along with the influence of annealing temperature on their structural, optical, and electrical characteristics. Copper and sulfur S are both lacking in all CMTS thin films. By using X-ray diffraction and X-ray photoelectron spectroscopy, results for the production of CMTS thin films with (Zinc-blend) structure were demonstrated. Lowering the temperature of sulfur reduces the energy gap and boosts crystallinity. At 530°C, the researcher found that the CMTS solar cell's maximum efficiency was 0.78% [73].

In 2020 Akash Sharma et al. Cu2MgSnS4 thin films were prepared as a solution using the Sol-gel process, and then was deposited on glass substrates by the Spin Coating method. The drying temperature was then varied by (250-400)°C to study the effects. According to the XRD

patterns, a tetragonal structure is created. With rising temperatures, the thin films' crystallinity also increased. Also, utilizing FE-SEM, the thin films' form remained consistent up until a drying temperature of 300 °C. But, when the drying temperature rose, various fractures and holes appeared in the produced films. When drying temperature rises, the projected energy gap values fall from 1.999 to 1.775 eV. [74].

Compound name	**Method**	**crystal structure**	**Band gab (eV)**	**References**
Cu_2CdSnS_4	Simple solution methed	Stannite	1.45	[78]
	Co- sputtering	Stannite	1.4	[79]
	Spin- coating	Stannite	1.25- 1.6	[80]
Cu_2ZnSnS_4	Electrostatic spraying methed	Kesterite	1.42-1.71	[81]
	Spin- caoting	Kesterite	1.7	[82]
	chemical spray pyrolysis	Kesterite	1.48-1.49	[83]
Cu_2CoSnS_4	Hot-injection	wurtzite		[84]
	Chemical spray pyrolysis	Stannite	1.4-1.7	[85]
	Spin Coating -Sol- gel	Stannite	1.45	[86]
Cu_2MgSnS_4	Hot-injection	Kesterite	1.63	[63]
	Spin- Coating	Stannite	1.775- 1.999	[87]
	Chemical spray pyrolysis	Kesterite	1.33- 1.91	[88]
	thermoelectric properties	Stannite-Kesterite	0.55- 1.10	[89]

Table 4: Characteristic parameters of the current best efficiency CZTS-based thin film solar cells with light absorber made by various methods.

METHOD	MATERIAL	N(%)	VOC (V)	JSC (MA/CM2)	FF	REF
RF magnetron sputtering	CZTS	6.77	0.61	17.9	0.62	[75]
Thermal evaporation	CZTS	6.8	0.587	17.8	0.65	[76]
Electrodeposition	CZTS	3.4	0.563	14.8	0.41	[77]
Hot injection	CZTSSe	7.2	0.42	30.4	0.527	[61]
Hydrazine	CZTSSe	9.67	0.516	28.6	0.65	[55]

Conclusions

Cu_2ZnSnS_4 has made great progress recently, proving that it is possible to create high-efficiency PV devices using inexpensive, environmentally friendly components. To deposit CZTS films, achieve of methods, including vacuum and nonvacuum methods, have been investigated. With

an efficiency of 6.77%, the vacuum-based spluttering technique have created CZTS films for thin films solar cells that are similar to the presentation of the film created via a quick thermal evaporation. Express vacuum thermal evaporation appears more than promising from an application standpoint for the large scale manufacture for thin film materials. The hydrazine-based particle-solution method has proven produce CZTS materials of the highest quality among non-vacuum preparation techniques. The thin films solar cells that use the hydrazine technique have an energy conversion efficiency of 9.66%, which supports this claim. A likely synthesis method to CZTS materials appears to be the hot-injection approach. The selenized CZTS nano crystal based thin films solar cells demonstrated a 7.2% alteration efficiency. Even while electro-deposition has been used commercially to effectively deposit CIGS and CdTe thin film , it could now able for compete with alternative methods for depositing high quality CZTS film . Most efficient solar cellS had a conversion rate of 3.4% and used electrodeposited CZTS material. Table 1 summarizes the key characteristics of the most advanced thin films solar cell produced using various techniques. Two highest efficiency cell are undoubtedly built using selenized CZTS light absorbance materials (CZTSSe). The cells' shorter circuit current concentration is almost twice that of the other cells made using CZTS materials. This is explained by the CZTSSe light absorber's wider spectrum sensitivity brought on by its smaller band gap energy. All CZTS based solar cells have an open circuit voltage of about 0.6 eV, which is significantly less than hypothetical value of 1.5 eV. The low Voc in those devices is likely caused by a high charge recombination rate. An in-depth examination of the device's electrical properties and charge-transfer kinetics is needed to pinpoint the specific physical causes of the low Voc. To improve the performance of thin film solar cells based on CZTS, it is essential to have a deeper understanding of the material's fundamental properties, particularly the types of faults and how they impact the material's properties. Thin film solar cells with high efficiency are often made of CZTS materials that are copper/zinc rich. Hence, a secondary phase should be present in the light absorbers. In order to optimize the manufacturing process and produce CZTS thin films by the correct properties, it is vital to identify these secondary phases and their impacts. XRD topography, SEM, UV-Vis, EIS, and I-V studies of the optical, morphological, electrochemical, and electrical aspects of CMTS movies. The band gap optimal

energy for stable kesterite Mg structure is 1.6 eV, according to XRD patterns. CMTS film have exceptional infrared and visible absorption. The 10^4 cm^{-1} order absorption coefficient was discovered. The usage of CMTS film photocurrent lighting as an absorbent layer for solar cell devices distinguishes it. In applications involving solar cells, it serves as an absorbent layer. Additionally, a thorough discussion of the sensing process for complicated impedance spectra is provided. These findings demonstrate the possible use of CMTS films in humidity sensors.

References

1. D. B. Mitzi, O. Gunawan, T. K. Todorov, K. Wang, S. Guha, Solar Energy Mater, The path towards a high-performance solution-processed kesterite solar cell, Solar Cells 95, 1421–1436(2011)
2. X. Song, X. Ji, M. Li, W. Lin, X. Luo, H. Zhang, A review on development prospect of CZTS based thin film solar cells, Int. J. Photoenergy 2014, 1–11, (2014)
3. W. Wei, W. Mark T, G. Oki, G. Tayfun, T. Teodor K, Z. Yu, M. David B, Device characteristics of CZTSSe thin-film solar cells with 12.6\% efficiency, Advanced energy materials, 4, 1301465(2014)
4. M. S. Kumar, S. P. Madhusudanan, S. K. Batabyal, Substitution of Zn in Earth-Abundant Cu2ZnSn (S, Se) 4 based thin film solar cells--A status review, Solar Energy Mater, Solar Cells, 185, 287–299(2018)
5. W. Zhao, G. Wang, Q. Tian, L. Huang, S. Gao, D. Pan, Solution-processed Cu2CdSn (S, Se) 4 thin film solar cells, Solar Energy Mater, Solar Cells, 133, 15–20, (2015).
6. P. R. Ramanujam, Zh. Su, X. Zeng, B. Tom, W. L. Shin, Sh. Sudhanshu, B. Sudip K, G. Oki, W. Lydia Helena, Photovoltaic effect in earth abundant solution processed Cu2MnSnS4 and Cu2MnSn (S, Se) 4 thin films, Solar Energy Mater, Solar Cells, 157, 867–873(2016)
7. M. Wei, Q. Du, R. Wang, G. Jiang, W. Liu, C. Zhu, Synthesis of new earth-abundant kesterite cu2mgsns4 nanoparticles by hot-injection method, Chem. Lett., 43, 1149–1151(2014)

8. C. Wang, S. Chen, J. Yang, L. Lang, H-J. Xiang, X. Gong, A. Walsh, S. Wei, Chem, Mater,26, 3411–3417(2014)

9. Y. Guo, W. Cheng, J. Jiang, S. Zuo, F. Shi, J. Chu, The structural, morphological and optical--electrical characteristic of Cu2XSnS4 (X: Cu, Mg) thin films fabricated by novel ultrasonic co-spray pyrolysis, Mater, Lett. 172, 68–71(2016)

10. S. Wagner, P. M. Bridenbaugh, Multicomponent tetrahedral compounds for solar cells, Journal of Crystal Growth, 39(1), 151–159(1977)

11. K. Ito, T. Nakazawa, Electrical and optical properties of stannite-type quaternary semiconductor thin films, Japanese Journal of Applied Physics, 27(11), 2094–2097 (1988)

12. K. Hironori, N. Masato, O. Takeshi, M. Shinichi, F. Masato, S. Toshiyuki, W. Taku, Rare-metal free thin film solar cell, in Proceedings of the Power Conversion Conference, 2, 1003–1006(1997)

13. H. Katagiri, N. Hando, S. Sasaguchi, S. Yokota, J. Hoshino, T. Ohashi, Preparation and evaluation of Cu_2ZnSnS_4 thin films by sulfurization of E-B evaporated precursors, Solar Energy Materials and Solar Cells, 49(1–4), 407–414(1997)

14. S. Chen, X. G. Gong, A. Walsh, S. H. Wei, Crystal and electronic band structure of Cu_2ZnSnX_4 (X = S and Se) photovoltaic absorbers: first-principles insights, Appl. Phys. Lett., 94, 041903(2009)

15. S. Chen, A. Walsh, Y. Luo, J. H. Yang, X.G. Gong, S. H. Wei, Wurtzite-derived polytypes of kesterite and stannite quaternary chalcogenide semiconductors, Phys. Rev. B 82, 195203(2010)

16. S. Chen, J.H. Yang, X.G. Gong, A. Walsh, S.H. Wei, Intrinsic point defects and complexes in the quaternary kesterite semiconductor Cu_2ZnSnS_4., Phys. Rev. B 81, 245204(2010)

17. D. Han, Y. Y. Sun, J. Bang, Y.Y. Zhang, H. B. Sun, X.B. Li, S.B. Zhang, Deep electron traps and origin of p-type conductivity in the earth-abundant solar-cell material Cu_2ZnSnS_4., Phys. Rev. B 87, 155206(2013)

18. C. Wang, S. Chen, J.H. Yang, L. Lang, H.J. Xiang, X.G. Gong, A. Walsh, S.H. Wei, Design of I_2–II–IV–VI_4 semiconductors through element substitution: the thermodynamic stability limit and chemical trend, Chem. Mater., 26, 3411(2014)

19. K. Jimbo, R. Kimura, T. Kamimura, S. Yamada, W.S. Maw, H. Araki, K. Oishi, H. Katagiri, Cu_2ZnSnS_4-type thin film solar cells using abundant materials, Thin Solid Films 515, 5997(2007)

20. S. Ahn, S. Jung, J. Gwak, A. Cho, K. Shin, K. Yoon, D. Park, H. Cheong, J. H. Yun, Determination of band gap energy (Eg) of $Cu_2ZnSnSe_4$ thin films: on the discrepancies of reported band gap values, Appl. Phys. Lett. 97, 021905(2010)

21. J. J. Scragg, P. J. Dale, L.M. Peter, Towards sustainable materials for solar energy conversion: preparation and photoelectrochemical characterization of Cu_2ZnSnS_4, Electrochem. Commun. 10, 639–642(2008)

22. M. Wei, Q. Du, R. Wang, G. Jiang, W. Liu, C. Zhu, Synthesis of new earth-abundant Kesterite Cu_2MgSnS_4 nanoparticles by hot-injection method, Chem. Lett., 43, 1149–1151(2014)

23. J. Krustok, R. Josepson, T. Raadik, M. Danilson, Potential fluctuations in $Cu_2ZnSnSe_4$ solar cells studied by temperature dependence of quantum efficiency curves, Physica B 405, 3186–3189(2010)

24. Ch. Shiyou ,W. Aron , Y. Ji-Hui , G. Xin-Gao ,S. Lin, Y. Ping-Xiong, Ch. Jun-Hao, W. Su-Huai, Compositional dependence of structural and electronic properties of $Cu_2ZnSn(S,Se)_4$ alloys for thin film solar cells, Physical Review B, 83, Article ID 125201(2011)

25. S. N. Sahu, R. K. Pandey, S. Chandra, Handbook of Semiconductor Electrodeposition, (Marcel Dekker, New York, 1996)

26. D. Lincot, Electrodeposition of semiconductors, Thin Solid Films, 487(1-2), 40–48 (2005)

27. L. Daniel, G. Jean-Franois, S. Taunier, D. Guimard, J. Sicx-Kurdi, A. Chaumont, O. Roussel, O. Ramdani, C. Hubert, JP. Fauvarque, Chalcopyrite thin film solar cells by electrodeposition, Solar Energy, 77(6), 725–737(2004)

28. D. Cunningham, M. Rubcich, D. Skinner, Cadmium telluride PV module manufacturing at BP solar, Progress in Photovoltaics: Research and Applications, 10(2), 159– 168 (2002)

29. B. E. McCandless, A. Mondal, R. W. Birkmire, Galvanic deposition of cadmium sulfide thin films, Solar Energy Materials and Solar Cells, 36(4), 369–379(1995)

30. J. J. Scragg, P. J. Dale, L. M. Peter, Towards sustainable materials for solar energy conversion: preparation and photoelectrochemical characterization of Cu_2ZnSnS_4., Electrochemistry Communications, 10(4), 639–642(2008)

31. J. J. Scragg, P. J. Dale, L. M. Peter, G. Zoppi, I. Forbes, New routes to sustainable photovoltaics: evaluation of Cu_2ZnSnS_4 as an alternative absorber material, Physica Status Solidi B, 245(9), 1772–1778(2008)

32. J. J. Scragg, D. M. Berg, P. J. Dale, A 3.2% efficient Kesterite device from electrodeposited stacked elemental layers, Journal of Electroanalytical Chemistry, 646(1-2), 52–59(2010)

33. A. Hideaki, K. Yuki, M. Aya, J. Kazuo, M. Win Shwe, K. Hironori, Y. Makoto, O. Koichiro, T. Akiko, Preparation of Cu_2ZnSnS_4 thin films by sulfurizing electroplated precursors, Solar Energy Materials and Solar Cells, 93(6-7), 996– 999(2009)

34. A. Hideaki, K.Yuki, J. Kazuo, M. Win Shwe, K. Hironori, Y. Makoto, O. Koichiro, T. Akiko, Preparation of Cu_2ZnSnS_4 thin films by sulfurization of co-electroplated Cu-Zn-Sn precursors, Physica Status Solidi C, 6(5), 1266–1268(2009)

35. S. Roland, A. Hlzing, J. Stefan, H. Rainer, V. Torsten, S. Jorg, A. Kirbs, E. Ahmed, M. Lux-Steiner, W. Alfons, The crystallisation of ¨ Cu_2ZnSnS_4 thin film solar cell absorbers from co-electroplated Cu-Zn-Sn precursors, Thin Solid Films, 517(7), 2465– 2468 (2009)

36. Q. Guo, H. W. Hillhouse, R. Agrawal, Synthesis of Cu_2ZnSnS_4 nanocrystal ink and its use for solar cells, Journal of the American Chemical Society, 131(33), 11672–11673 (2009).

37. S. Ahmed, K. B. Reuter, O. Gunawan, L. Guo, L. T. Romankiw, H. Deligianni, A high efficiency electrodeposited Cu_2ZnSnS_4 solar cell, Advanced Energy Materials, 2(2), 253–259(2012)

38. N. M. Shinde, D. P. Dubal, D. S. Dhawale, C. D. Lokhande, J. H. Kim, J. H. Moon, Room temperature novel chemical synthesis of Cu_2ZnSnS_4 (CZTS) absorbing layer for photovoltaic application, Materials Research Bulletin, 47(2), 302– 307(2012)

39. S. S. Mali, P. S. Shinde, C. A. Betty, P. N. Bhosale, Y. W. Oh, P. S. Patil, Synthesis and characterization of Cu_2ZnSnS_4 thin films by SILAR method, Journal of Physics and Chemistry of Solids, 73(6), 735–740(2012)

40. M. Sawanta S, P. Bharmana M, B. Chirayath A, B. Popatrao N, Oh, Young Woo, J. Sandesh R, D. Rupesh S, M. Yuan-Ron, P. Pramod S, Novel synthesis of kesterite Cu_2ZnSnS_4 nanoflakes by successive ionic layer adsorption and reaction technique: characterization and application, Electrochimica Acta, 66, 261–221(2012)

41. W. Tsukasa, Sh. Tomokazu, T. Shin, F. Tatsuo, M. Tomoyoshi, J. Kazuo, K. Hironori, 6% Efficiency Cu_2ZnSnS_4 - based thin film solar cells using oxide precursors by open atmosphere type CVD, Journal of Materials Chemistry, 229(9), 4021–4024(2012)

42. N. Nakayama, K. Ito, Sprayed films of stannite Cu_2ZnSnS_4., Applied Surface Science, 92, 171–175(1996)

43. N. Kamoun, H. Bouzouita, B. Rezig, Fabrication and characterization of Cu_2ZnSnS_4 thin films deposited by spray pyrolysis technique, Thin Solid Films, 515(15), 5949–5952(2007)

44. Y. B. K. Kumar, G. S. Babu, P. U. Bhaskar, V. S. Raja, Preparation and characterization of spray-deposited Cu_2ZnSnS_4 thin films, Solar Energy Materials and Solar Cells, 93(8), 1230–1237(2009)

45. Y. B. K. Kumar, G. S. Babu, P. U. Bhaskar, V. S. Raja, Effect of starting-solution pH on the growth of Cu_2ZnSnS_4 thin films deposited by spray pyrolysis, Physica Status Solidi A, 206(7), 1525–1530(2009)

46. T. Prabhakar, J. Nagaraju, Ultrasonic spray pyrolysis of CZTS solar cell absorber layers and characterization studies, In: Proceedings of the 35th IEEE Photovoltaic Specialists Conference, (PVSC '10), 1964–1969, June (2010)

47. M. Souli, R. Engazou, L. Ajili, N. Kamoun-Turki, Physical properties evolution of sprayed Cu_2MgSnS_4 thin films with growth parameters and vacuum annealing, Superlattices and Microstructures, 147, 106711(2020)

48. A. Hammoud, B. Yahmadi, M. Souli, S. A. Ahmed, L. Ajili, N. Kamoun-Turki, Effect of sulfur content on improving physical properties of new sprayed Cu_2MgSnS_4 thin films compound for optoelectronic applications, The European Physical Journal Plus, 137(2) 1-12(2022)

49. K. Tanaka, N. Moritake, H. Uchiki, Preparation of Cu_2ZnSnS_4 thin films by sulfurizing sol-gel deposited precursors, Solar Energy Materials and Solar Cells, 91(13), 1199–1201(2007)

50. K. Tanaka, M. Oonuki, N. Moritake, H. Uchiki, Cu_2ZnSnS_4 thin film solar cells prepared by non-vacuum processing, Solar Energy Materials and Solar Cells, 93(5), 583–587(2009)

51. K. Tanaka, Y. Fukui, N. Moritake, H. Uchiki, Chemical composition dependence of morphological and optical properties of Cu_2ZnSnS_4 thin films deposited by sol-gel sulfurization and Cu_2ZnSnS_4 thin film solar cell efficiency, Solar Energy Materials and Solar Cells, 95(3), 838–842(2011)

52. BS. Pawar, SM. Pawar, SW. Shin, DS. Choi, CJ. Park, SS. Kolekar, JH. Kim, Effect of complexing agent on the properties of electrochemically deposited Cu_2ZnSnS_4 (CZTS) thin films, Applied Surface Science, 257(5), 1786–1791(2010)

53. L. Yufeng, Ge. Meiying, Y. Yang, S. Yan, W. Yizheng, Ch. Xin, D. Ning, Colloidal Cu_2ZnSnS_4 nanocrystals generated by a facile route using ethylxanthate molecular precursors, Physica Status Solidi, 5(3), 113–115(2011)

54. A. Fischereder, T. Rath, W. Haas, H. Amenitsch, J. Albering, D. Meischler, S. Larissegger, M. Edler, R. Saf, F. Hofer, Investigation of Cu_2ZnSnS_4 formation from metal salts and thioacetamide, Chemistry of Materials, 22(11), 3399–3406(2010)

55. K. Todorov, K. B. Reuter, D. B. Mitzi, High-efficiency solar cell with earth-abundant liquid-processed absorber, Advanced Materials, 22(20), E156–E159(2010)

56. S. C. Riha, B. A. Parkinson, A. L. Prieto, Solution-based synthesis and characterization of Cu_2ZnSnS_4 nanocrystals, Journal of the American Chemical Society, 131(34), 12054–12055(2009)

57. Q. J. Guo, H. W. Hillhouse, R. Agrawal, Synthesis of Cu_2ZnSnS_4 nanocrystal ink and its use for solar cells, Journal of the American Chemical Society, 131(33), 11672–11673(2009)

58. C. Steinhagen, M. G. Panthani, V. Akhavan, B. Goodfellow, B. Koo, B. A. Korgel, Synthesis of Cu_2ZnSnS_4 nanocrystals for use in low-cost photovoltaics, Journal of the American Chemical Society, 131(35), 12554–12555(2009)

59. T. Kameyama, T. Osaki, K. I. Okazaki, T. Shibayama, A. Kudo, S. Kuwabata, T. Torimoto, Preparation and photoelectrochemical properties of densely immobilized Cu_2ZnSnS_4 nanoparticle films, Journal of Materials Chemistry, 20(25), 5319–5324(2010)

60. P. C. Dai, X. N. Shen, Z. J. Lin, Z. Y. Feng, H. Xu, J. H. Zhan, Band-gap tunable $(Cu_2Sn)_x/3Zn_{1-x}S$ nanoparticles for solar cells, Chemical Communications, 46(31), 5749–5751(2010)

61. Q. Guo, G. M. Ford, W. C. Yang, B. C. Walker, E. A. Stach, H. W. Hillhouse, R. Agrawal, Fabrication of 7.2% efficient CZTSSe solar cells using CZTS nanocrystals, Journal of the American Chemical Society, 132(49), 17384– 17386(2010)

62. X. T. Lu, Z. B. Zhuang, Q. Peng, Y. D. Li, Wurtzite Cu_2ZnSnS_4 nanocrystals: a novel quaternary semiconductor, Chemical Communications, 47(11), 3141–3143(2011)

63. W. Ming, D. Qingyang, W. Rong, J. Guoshun, L. Weifeng, Z. Changfei, Synthesis of new earth-abundant kesterite Cu_2MgSnS_4 nanoparticles by hot-injection method, Chemistry Letters, 43.7, 1149-1151(2014)

64. A. V. Moholkar, S. S. Shinde, A. R. Babar, K. U. Sim, Y.B. Kwon, K. Y. Rajpure, P.S. Patil, C. H. Bhosale, J. H. Kim, Development of CZTS thin films solar cells by pulsed

laser deposition: influence of pulse repetition rate, Solar Energy, 85(7), 1354– 1363 (2011)

65. N. Muhunthan, O. P. Singh, S. Singh, V. N. Singh, Growth of CZTS thin films by cosputtering of metal targets and sulfurization in H_2S, International Journal of Photoenergy, 2013, Article ID 752012, 7 pages, (2013)

66. K. Tanaka, M. Oonuki, N. Moritake, H. Uchiki, Cu_2ZnSnS_4 thin film solar cells prepared by non-vacuum processing, Solar Energy Materials and Solar Cells, 93(5), 583–587(2009)

67. K. Tanaka, Y. Fukui, N. Moritake, H. Uchiki, Chemical composition dependence of morphological and optical properties of Cu_2ZnSnS_4 thin films deposited by sol-gel sulfurization and Cu_2ZnSnS_4 thin film solar cell efficiency, Solar Energy Materials and Solar Cells, 95(3), 838–842(2011)

68. Q. Guo, G. M. Ford, W. C. Yang, B. C. Walker, E.A. Stach, H. W. Hillhouse, R. Agrawal, Fabrication of 7.2% efficient CZTSSe solar cells using CZTS nanocrystals, Journal of the American Chemical Society, 132(49), 17384– 17386(2010)

69. T. K. Todorov, K. B. Reuter, D. B. Mitzi, High-efficiency solar cell with earth-abundant liquid-processed absorber, Advanced Materials, 22(20), E156–E159 (2010)

70. T. Todorov, O. Gunawan, S. J. Chey, T. G. De Monsabert, A. Prabhakar, D. B. Mitzi, Progress towards marketable earthabundant chalcogenide solar cells, Thin Solid Films, 519(21), 7378–7381(2011)

71. B. D. Mitzi, K. T. Todorov, O. Gunawan, M. Yuan, Q. Cao, W. Liu, B. K. Reuter, M. Kuwahara, K. Misumi, J. A. Kellock, Torwards marketable efficiency solution-processed kesterite and chalcopyrite photovoltaic devices, In: Proceedings of the 35th IEEE Photovoltaic Specialists Conference (PVSC ’10), pp. 640–645, June (2010).

72. D. A. R. Barkhouse, O. Gunawan, T. Gokmen, T. K. Todorov, D. B. Mitzi, Device characteristics of a 10.1% hydrazineprocessed $Cu_2ZnSn(Se,S)_4$ solar cell, Progress in Photovoltaics: Research and Applications, 20(1), 6–11(2012)

73. G. Yang, X. Zhai, Y. Li, B. Yao, Z. Ding, R. Deng, H. Zhao, L. Zhang, Z. Zhang, Synthesis and characterizations of Cu_2MgSnS_4 thin films with different sulfuration temperatures, Mater. Lett., 242, 58–61(2019)

74. A. Sharma, P. Sahoo, A. Singha, S. Padhan, G. Udayabhanu, R. Thangavel, Efficient visible-light-driven water splitting performance of sulfidation-free, solution processed Cu_2MgSnS_4 thin films: Role of post-drying temperature, Sol. Energy, 203, 284–295 (2020)

75. H. Katagiri, K. Jimbo, S. Yamada, T. Kamimura, W. Maw, T. Fukano, T. Ito, T. Motohiro, Enhanced conversion efficiencies of Cu_2ZnSnS_4 -based thin film solar cells by using preferential etching technique, Applied Physics Express, 1(4), Article ID 041201, 2 pages, (2008)

76. K. Wang, O. Gunawan, T. Todorov, B. Shin, S. J. Chey, N. A. Bojarczuk, D. Mitzi, S. Guha, Thermally evaporated Cu_2ZnSnS_4 solar cells, Applied Physics Letters, 97(14), Article ID 143508(2010)

77. A. Ennaoui, M. Lux-Steiner, A. Weber, D. Abou-Ras, I. Kotschau, H.W. Schock, R. Schurr, A. Holzing, S. Jost, R. Hock, Cu_2ZnSnS_4 thin film solar cells from electroplated precursors: novel low-cost perspective, Thin Solid Films, 517(7), 2511–2514 (2009)

78. H. Guan, Y. Shi, F. Yu, X. Wang, H. Hou, Quaternary Cu_2CdSnS_4 nanoparticles synthesized by microwave irradiation method, Micro & Nano Letters, 9(4), 251-252 (2014)

79. H. Guo, Y. Li, X. Fang, K. Zhang, J. Ding, N. Yuan, Co-sputtering deposition and optical-electrical characteristic of Cu_2CdSnS_4 thin films for use in solar cells, Materials Letters, 162, 97-100 (2016)

80. A. Odeh, Y. Al-Douri, R. M. Ayub, M. Ameri, A. Bouhemadou, D. Prakash, K. D. Verma, Optical analysis of lens-like Cu_2CdSnS_4 quaternary alloy nanostructures, Applied Physics A, 122(10), (2016)

81. L. Chen, C. Park, Effects of annealing temperature on Cu_2ZnSnS_4 (CZTS) films formed by electrospray technique, Korean Journal of Chemical Engineering, 34(4), 1187-1191 (2017)

82. E. M. Mkawi, Y. Al-Hadeethi, E. Shalaan, E. Bekyarova, Solutionprocessed sphere-like Cu_2ZnSnS_4 nanoparticles for solar cells: effect of oleylamine concentration on properties, Applied Physics A, 126(1), (2020)

83. M. AS, K. SA, K. RS, D. RJ, Chemical Spray Deposited Nickel Sulphide Thin Films for Supercapacitor applications, Journal of Science and Engineering, Special Issue A1, 195-198(2017)

84. Gupta A, Mokurala K, Kamble A, Shankar S, Mallick S, Bhargava P. Synthesis and characterization of magnetic semiconducting Cu_2CoSnS_4 nanoparticles, In: AIP Conference Proceedings, (Vol. 1665, No. 1, p. 140022), (2015).

85. Maldar PS, Mane AA, Nikam SS, Giri SD, Sarkar A, Moholkar AV. Correction to: Temperature dependent properties of spray deposited Cu_2CoSnS_4 (CCTS) thin films, Journal of Materials Science: Materials in Electronics, 28(24),18897(2017)

86. Sharma A, Thangavel R. Cost-effective fabrication of Cu_2CoSnS_4 thin films for photovoltaic applications, In: 3rd International Conference on Microwave and Photonics (ICMAP) (pp. 1-2). IEEE, (2018)

87. A. Sharma, P. Sahoo, A. Singha, S. Padhan, G. Udayabhanu, and R. Thangavel, Efficient visible-light-driven water splitting performance of sulfidation-free, solution processed Cu_2MgSnS_4 thin films: Role of post-drying temperature, Sol. Energy, 203, 284–295 (2020)

88. M. Souli, R. Engazou, L. Ajili, N. Kamoun-Turki, Physical properties evolution of sprayed Cu_2MgSnS_4 thin films with growth parameters and vacuum annealing, Superlattices and Microstructures, 147, 106711(2020)

89. S. Sonu, P. Kumar, Quaternary semiconductors Cu_2MgSnS_4 and $Cu_2MgSnSe_4$ as potential thermoelectric materials, Journal of Physics Communications, 1.4, 045014, (2017)